IJHSR
ijhighschoolresearch.org
RESEARCH ARTICLE

An Integrated Lock-in Amplifier and Near Infrared Method for Finding Fruits Fully Behind Leaves in a Homemade Testbed

Aiden Xu

Winter Springs High School, 130 Tuskawilla Rd, Winter Springs, FL 32708, USA; goaidenxu@gmail.com

ABSTRACT: Detecting fully occluded objects is of interest for various practical problems, such as harvesting and yield prediction in farming, which are physically demanding and heavily labor-dependent. Many approaches have been explored by researchers aiming to solve this problem. However, they are ineffective due to inherent challenges: the strength of signals reflected from hidden objects is weak, and those signals are always buried in high-magnitude noise. In this study, a method combining near-infrared (NIR) and lock-in-amplifier (LIA) techniques is proposed to tackle these challenges. Two questions are answered. Can a fully covered fruit be detected purely based on reflected NIR signals? Can LIA extract reflected signals from high-magnitude noise? This study addresses these questions from theoretical and experimental points of view, including NIR photon particle propagation, LIA in the image format, low-cost experiment apparatus, etc. In total, 268 videos were collected over 134 valid experiments with tomatoes and cucumbers as objects. Both alternate hypotheses were validated and answered.

KEYWORDS: Embedded Systems, Sensors, Occluded Fruit Detection, Near Infrared, Lock-in-Amplifier.

Introduction

Finding what's behind or hidden in leaves is a key step in many applications. For example, many farming activities are labor-intensive and physically demanding, such as yield prediction, leaf thinning, harvesting, and pesticide applications.[1-4] Among them, harvesting is mostly done manually,[4] especially for fruit crops like tomatoes, cucumbers, and strawberries. However, labor is in short supply in the US,[5] which means more robots are needed. For a robot to effectively conduct those tasks currently done by humans, it needs to know if there is something (e.g., fruit, flower, or peduncle) behind dense leaves.

In the past decade, many researchers have investigated different methods to solve the aforementioned problems. Most of them utilized vision-based, artificial intelligence (AI) methods.[1, 6-12] A method to detect tomatoes using visible light cameras and machine learning was investigated as well.[12] Another study used a leaf blower to mechanically expose hidden apples so a LIDAR could be used more effectively to detect them.[1] However, to date, none of them have been highly successful. The main issues are: (i) the reflected signal from hidden fruits is weak, and (2) the reflected signal is buried in high magnitude noise. The author also noticed that, very recently, researchers [13, 14] used millimeter wave radar techniques in finding fruits behind leaves[14] with relatively higher cost, lower reflectivity on soft material surfaces, and the need for a specialized imaging system.

In this study, a method combining near-infrared (NIR) and lock-in-amplifier (LIA) [15] in the image format is proposed to address these issues. There are two sets of hypotheses. In Hypothesis Set 1, "effective" means the method is effective in detecting the presence of an object fully hidden behind leaves. "Scenario 1" represents a scenario with a fully occluded object, while "Scenario 2" represents a scenario without such an object. In Hypothesis Set 2, "effective" means the proposed method is better than the simple image subtraction method (the control group) in detecting an object.

Null Hypothesis 1 (N1): If in more than 30% of the experiments, the reflected NIR signal in "Scenario 1" is NOT significantly different from that of "Scenario 2", then the proposed method is NOT "effective".

Alternative Hypothesis (AH1): If in more than 70% of the experiments, the reflected NIR signal in "Scenario 1" is significantly higher than that of "Scenario 2", then the proposed method is "effective".

Null Hypothesis 2 (N2): If in more than 30% of the experiments, the percentage difference of the LIA technique is NOT higher than the simple subtraction method, then the proposed method is not "effective".

Alternative Hypothesis 2 (AH2): If in more than 70% of the experiments, the percentage difference of the LIA technique is higher than that of the simple subtraction method, then the proposed method is "effective".

The research conducted to validate those hypotheses consists of three main parts. The first part is to select the diodes with the best wavelength considering cost, product availability, and optical properties on leaves and fruits. The second part is to create an innovative, in-house testbed: the "emitter" box (producing NIR signals modulated with the Pulse Width Modulation - PWM), the "orchard" box (housing leaves and fruit), and the "phone holder" (a stable base for a cell phone to detect NIR signals and record experiments). The third part, LIA in the image format, is the most innovative one. Software for signal generation and data analysis was also developed.

The contributions of this study are as follows. As far as the author knows, there are two technical contributions. (i) The test apparatus can conduct experiments to validate the research hypotheses despite costing much less than any optical equipment in research laboratories. (ii) It is the first time a combined

DOI: 10.36838/v8i2.1

technology of NIR and LIA has been tried in detecting fully occluded fruits. On a broader scale, this research has the potential to reduce labor dependence and enable more efficient robotic operations in harvesting, yield prediction, etc. If combined with different electromagnetic waves, this research can benefit an even wider range of applications, e.g., robot motion in off-road environments and medical imaging,[16] etc.

The paper is organized as follows. Firstly, I will discuss the theoretical background, test apparatus, data analysis tools, and experiments. Then, the experimental data and findings will be shown. Discussions, limitations, and conclusions are given in the end.

Methods

Theoretical Background:

1. NIR photon particle propagation and detection

Figure 1 shows the sketch of how the NIR photon particles propagate in the custom-designed experiment apparatus (discussed later). D, I_o, A_{out}, and A_{in} represent the detector efficiency, initial NIR intensity, signal attenuation outside of leaves, and signal attenuation inside of leaves. The leaf transmissivity, object reflectability, and leaf reflectability are denoted by L_T, O_R, and L_R, respectively.[2] $I_{F_{in}}$ and $I_{F_{out}}$ are the reflected NIR signal intensity detected by the camera.

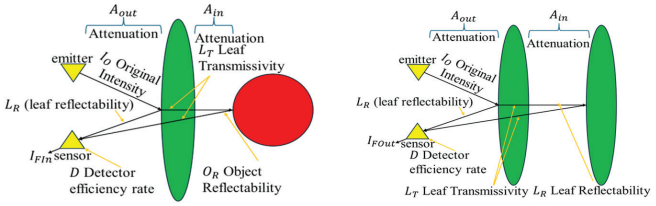

Figure 1: NIR signal propagation. (Left) with a fruit fully behind leaves and (right) no fruit behind. In this experiment setup, the PWM-modulated NIR signals are emitted, and a camera or detector receives the reflected NIR signals. There are two paths for the reflected signals: (i) directly reflected by the leaves and (ii) transmitted through leaves and reflected by the fruit (left) or leaves (right). Based on this experiment sketch, an equation can be derived to determine the difference in reflected signal intensities between the cases with and without a hidden fruit.

The NIR signal strength when a fruit is behind leaves, $I_{F_{in}}$, is derived as

$$I_{FIn} = D\left[(I_O A_{out}^2 {L_T}^2 A_{in}^2 O_R) + (I_O A_{out}^2 L_R)\right] \quad (1)$$

which considers the NIR signal reflected directly from the leaves and the NIR transmitted through leaves, bounced back from the hidden fruits, and then transmitted through the leaves again.

Similarly, the NIR signal strength when there is no fruit behind leaves, $I_{F_{out}}$, is derived as

$$I_{FOut} = D\left[(I_O A_{out}^2 {L_T}^2 A_{in}^2 L_R) + (I_O A_{out}^2 L_R)\right] \quad (2)$$

Therefore, the difference between $I_{F_{out}}$ and $I_{F_{in}}$, represented by ΔI, is derived as

$$\Delta I = I_{FIn} - I_{FOut} = D I_O L_T^2 A_{out}^2 A_{in}^2 (O_R - L_R) \quad (3)$$

One way to increase ΔI is to increase the initial intensity I_o; therefore, 20 diodes are used based on the test apparatus volume. Secondly, the wavelength with a high L_T, low L_R, and a high O_R should be chosen. Based on the optical experiment, the Gikfun® 940nm diodes were adopted (also low cost).

2. Lock-in amplifier in the image format

The LIA technique has been widely used to extract useful but weak signals buried from large magnitude of noise that with frequencies different from the reference signal.[15] Figure 2 shows how the LIA method is customized in the image format for the custom-designed experiment. In the scenarios of fruits being fully hidden behind leaves, as shown in Eq. 3, the reflected NIR signal differences between the scenarios with and without hidden fruits are very small.

The Arduino instructs the NIR diodes to emit a signal A_I modulated with a PWM square wave in its Fourier series $\sum_{i=1}^{n} m_i \sin[(2i-1)\omega t + \phi]$.[17] Here, A_I can be $I_{F_{in}}$ (Eq. 1) or $I_{F_{out}}$ (Eq. 2), ω is the foundational frequency, t is the time, and ϕ is the phase angle.[17] $m_i = 4/[\pi(2i-1)]$,$i=1, \ldots, n$, is the coefficient in the Fourier series expansion with n harmonics.[17] The detected signal S_I is

$$S_I = \{A_I \sum_{i=1}^{n} m_i \sin[(2i-1)\omega t + \phi] + N_I\} \quad (4)$$

where N_I is noise (e.g., random, specific frequency). As shown in Figure 2, the signal S_I goes through an average filter to remove random noise, and is then multiplied by a reference signal R (PWM) to output signal S_O. After that the signal SO goes through a Butterworth low-pass filter (LPF),[18] and the remaining DC component is S_{OL}. As shown in the derivation in Appendix A, A_I equals S_{OL}. The equations used in the custom designed experiment are shown in Appendix A. The process of using LIA is illustrated in Figure 2.

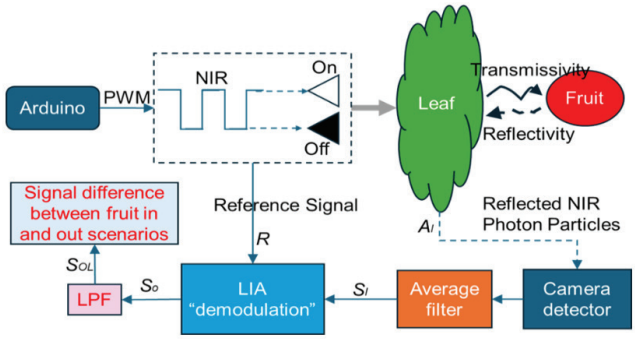

Figure 2: Signal flow chart in the experiments and data analysis. The NIR diodes will emit NIR signals which are modulated by PWM. The camera will detect reflected NIR signals. An average filter is first used to remove random noise, and then the resultant signal modulated with the reference signal through the LIA demodulation. After an LPF, the reflected NIR signal is calculated. As shown in later experiments, this method is effective in validating the alternative hypotheses.

Test Apparatus:

The test apparatus went through five design iterations, and only the final version is shown here.

1. NIR emitter box design:

As shown in Figure 3-left side, the "emitter" box produces a NIR signal modulated with PWM, has an access point to the Arduino and an external button to control signal starting, holds all necessary circuitry, and reflects minimal light to reduce noise. The "emitter" box is based in a 25.38x17.77x17.77 cm^3 wooden box, and 20 holes were drilled on one side for the diodes. The circuits are controlled by an Arduino Mega®. A button is present for controlling the signal's start. Each of the 4 breadboards connects with five diodes. The diodes are arranged in two circles (Figure 3-right side). The inner circle has 8 diodes, and the outer has 12 diodes. This pattern was determined by considering the limitations coming from size and volume constraints of the emitter box, diodes, and wires. To minimize reflected light, all exterior surfaces except the back were painted black. On each breadboard, one side hosts two diodes and the other hosts three. For the side with two, since each diode requires 1.2V and the Arduino outputs 5V, 2.6V is taken by the resistor. Since the diode's working current is 30mA, an 87Ω resistor is needed for that part of the circuit. Following a similar calculation, the resistor used in the 3-diode circuit is 47Ω. Since the legs of a diode were too short to reach the breadboard, soldering jumper cables is required.

2. Orchard box design and phone holder:

The "orchard" box must house leaves and fruit and keep them in their spots during an experiment, as well as minimize light reflection. Thus, the "orchard" box, shown in Figure 3 (left side), has three horizontal lines of string across the front. The topmost is where leaves are attached; the other two prevent the leaves from curling inward. Behind them is a raised platform, where the object is placed. The orchard box inside is covered in black foam to minimize light reflecting off it.

The "phone holder" needs to provide a low-cost, stable base for a cell phone to detect reflected NIR signals and record experiments. As such, it is built of plastic building bricks. It is hollow in the middle, for holding and steadying the cell phone to keep it in the same place while recording in different experiments. The cell phone's brightness is set to the minimum to avoid emitting excess light.

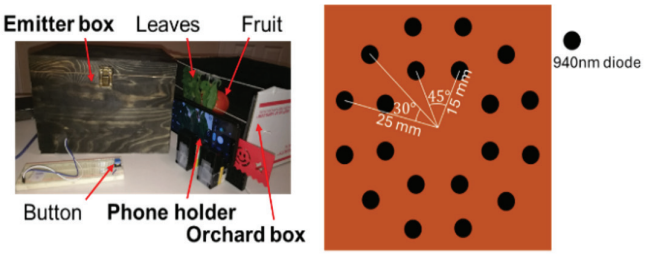

Figure 3: Test apparatus (left) and the layout of diodes (right). On the left, the test apparatus includes an "emitter" box for NIR signal generation, an "orchard" box holding leaves and fruit, and a phone holder to support the camera. On the right, there are 20 NIR diodes arranged in two concentric circles to increase the signal intensity. As a result, the apparatus is efficient and low-cost, and can be easily made from materials found around the household.

Data Analysis and Software:

About 1,600 lines of code (six codes) were programmed in Arduino® and MATLAB®.

1. NIR signal modulated with PWM:

(Code 1) The Arduino® code is to instruct the diodes to emit NIR signals modulated with PWM (6 seconds or 10 seconds, with 10 periods for each experiment). The signal is turned on by pressing a button to sync signal generation with video recording.

2. Data analysis tools:

(Code 2) Before the data analysis tools are applied, three signals (fruit in and out NIR signals and the PWM reference signal) should be synchronized. The data retrieval code extracts the RGB values of pixels and takes each frame's average RGB values, acting as an average filter.

(Code 3) The first data analysis method is the simple subtraction method, serving as the "control" group. This method simply subtracts the image without a fruit from the image with a fruit. Code 4 and Code 5 are for the LIA and the LIA with a Butterworth LPF.[18] Code 6 is to implement a dual LIA method with LPF, and interested readers can find how a dual LPF works.[15]

Experiments:

1. Leaf and fruit optical properties experiment:

The optical property experiment was conducted at a University of Central Florida laboratory using an Evolution 220® spectrophotometer following the procedure in Figure 4. According to the experiment results and following Eq. (3), the 940nm wavelength diodes were selected.

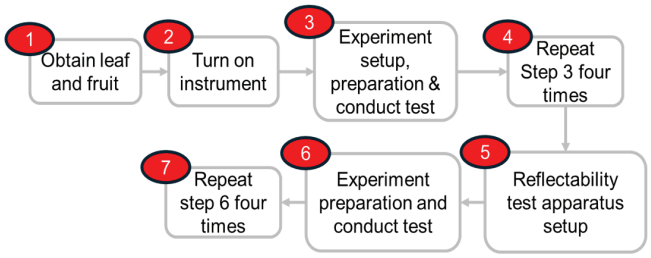

Figure 4: Procedure of leaf and fruit optical property experiment. The procedure follows the guideline of the instrument, and experiments were conducted to check the reflectivity and transmissivity of fruit and its corresponding leaf. It was found that the 940nm wavelength diode would be ideal, because (i) for leaves it has relatively low absorption and reflectability, and high transmissivity, and (ii) for fruits it has low absorption and transmissivity and high reflectability, in addition to being low-cost.

2. Experiments of detecting fully covered objects:

As shown in Figure 5, first, obtain enough leaves to cover the front of the "orchard" box and a fruit. The leaves are taped to the topmost string, and the fruit is placed on the platform. Next, the "emitter", "orchard", and "phone holder" are arranged properly, with 2.54 cm or 0 cm of distance between the "emitter" and "orchard" boxes, with the "phone holder" wedged between the two. The computer is then connected to the Arduino, and the PWM signal period is set to either 6 or 10 seconds. Both the record button and the signal start button

DOI: 10.36838/v8i2.1

are pressed at the same time to start. Once 10 periods are over, stop the phone recording. Now, remove the fruit and repeat the process. Each experiment consists of two scenarios: one with an object fully covered by leaves and the other without such an object; and this is counted as one independent replicate.

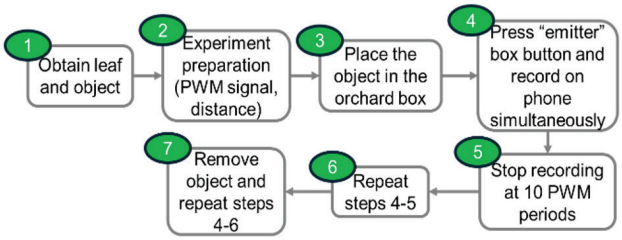

Figure 5: Experiment procedure of detecting fully occluded fruits. As shown in the results below, the experiment procedure is effective at validating the alternate hypotheses.

Result and Discussion

Experiment Data:

A total of 178 experiments were conducted over 20 weeks, and 356 videos were collected. However, not all of them were used, as some were invalidated due to an experiment setup error causing high amounts of ambient noise, while incorrect types of leaves were used in other invalidated experiments. In the end, 134 experiments and their 268 videos were used in the data analysis.

Experiment Results:

Table 1 shows the number of experiments that fulfill the requirements of AH1 (a), AH2 (b), and both (c), respectively, in the format of (a, b, c). For example, (36, 37, 34) represents the number of experiments using tomato fruit that validated AH1, AH2, and both, respectively. In 107 out of 134 experiments, both alternate hypotheses are validated (Table 1).

Table 1: Successful experiments in validating the alternate hypotheses. Experiments were conducted for four settings: PWM periods (6s or 10s) and the distance between "emitter" and "orchard" (0cm or 1" (2.54cm)). A total of 134 experiments are shown here. The number of experiments that can validate AH1, AH2, and both are listed in the form of (a, b, c), respectively. Both AH1 and AH2 are supported because the percentages of the successful detections are above 70%.

Experiments (AH1, AH2, Both)					
Scenarios	1" 6s	1" 10 s	0" 6s	0" 10s	Total
Tomato	(11, 11, 10)	(8,8,8)	(10, 10, 9)	(7,8,7)	(36, 37,34)
Tomato peduncle	(6, 6, 6)	(6, 6, 6)	(4, 6,4)	(6, 6, 6)	(22, 24, 22)
Cucumber	(9,10,7)	(22, 15, 14)	(12, 8, 8)	(14, 14, 14)	(57, 47, 43)
Cucumber peduncle	(2, 2, 2)	(2, 2, 2)	(2, 2, 2)	(4, 2, 2)	(10, 8, 8)

The following figures show the detailed experiment results of different fruits and different experiment configurations. In Figures 6 and 7, it is obvious that the LIA methods extracted significantly higher signals as compared to the simple subtraction method when a fruit is there. However, the difference between when peduncles are there or not is not obvious (Figure 8).

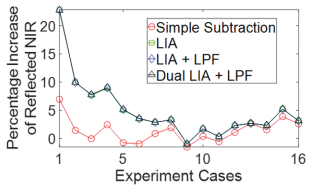

Figure 6: % increase of reflected NIR (2.54 cm distance, 6s period) with a tomato fruit. As compared with the control group (using the simple subtraction method), the LIA methods have larger percentage increases when there is a fully hidden fruit.

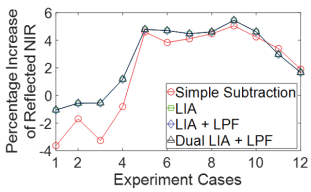

Figure 7: % increase of reflected NIR (2.54 cm distance, 6s period) with a cucumber. Similar findings are found as in Figure 6.

Figures 9 and 10 show the overall detection rates of different fruits and peduncles. The detection rate for tomatoes is above 87% (Figure 10) as compared to above 48% in the control group (Figure 9), signifying that the proposed method is more effective. In addition, since the peduncle detection rates are below 20%, the proposed method can differentiate between fruits and peduncles.

Statistical tools are used to analyze results. In Figures 11 and 12, the mean values in both the control and experiment groups are positive and mostly above 1% when detecting hidden fruits, meaning AH1 is supported. In addition, the mean value bars are located higher when using the LIA method as opposed to the simple subtraction method, supporting AH2. Those observations are not obvious when peduncles are used, meaning the proposed method can tell the difference between fruits and peduncles. The trend in standard deviation values in those figures is similar for both control and experiment groups. However, that is because in this custom designed experiment scenario, the majority of noise is random noise, which is filtered out by an average filter used in both SSM and LIA methods. Thus, their standard deviation trends are similar. However, since the LIA method can remove noise with frequencies different from the reference signal, its results are slightly better, and thus AH2 is supported.

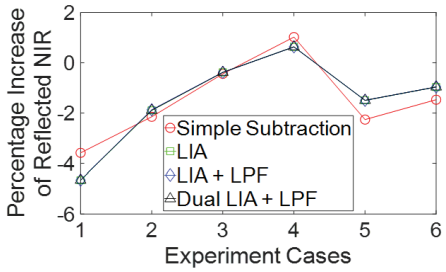

Figure 8: % increase of reflected NIR (2.54 cm distance, 6s period) with tomato peduncles. Null hypotheses are supported because the percentage difference between the control group (the simple subtraction method) and the proposed LIA method is not significant. However, this is as expected, since it means that the method can differentiate between fruits and peduncles.

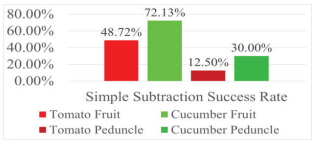

Figure 9: The overall success rate of the simple subtraction method. The detection rate in hidden fruit cases is significantly higher than those of peduncle cases.

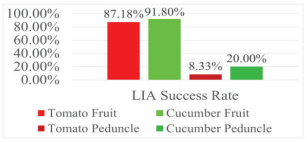

Figure 10: The overall success rate of the LIA method. The detection rate when using the proposed LIA method is much higher than those of the simple subtraction method, which validates alternate hypothesis 2.

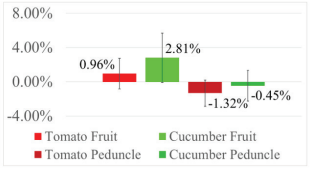

Figure 11: Mean +/- standard deviation percentage increase of reflected NIR (simple subtraction). The mean values of signal percentage increases are 0.96% and 2.81% for tomato and cucumber cases, respectively, meaning AH1 is supported.

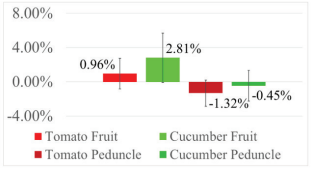

Figure 12: Mean +/- standard deviation percentage increase of reflected NIR (LIA). As compared with the control group, the proposal LIA method can achieve a much higher signal percentage increase.

The following figures show the t-test between the simple subtraction and LIA methods. In both Figure 13 and Figure 14, the t-stat is less than the negative t-critical two-tail, meaning that LIA is better than the simple subtraction method, rejecting N2 and supporting AH2.

Hypothesized Mean Difference	0.01
t Stat	-8.10701
t Critical two-tail	3.588363
t Stat < t Critical two-tail (negative), so reject NULL	

Figure 13: T-test for the simple subtraction and LIA methods (tomato). Here, the t-stat value (-8.10701) is less than -3.588363, meaning N2 is rejected and AH2 is supported.

Hypothesized Mean Difference	0.01
t Stat	-3.92496
t Critical two-tail	3.586372
t Stat < t Critical two-tail (negative), so reject NULL	

Figure 14: T-test for the simple subtraction and LIA methods (cucumber). Here, the tstat number (-3.92496) is less than the negative t-critical two tail value (- 3.586372). Therefore, AH2 is supported and N2 is rejected.

The following two figures (Figure 15 and Figure 16) show the ANOVA tests between different experiment configurations: namely, 2.54 cm-6s, 2.54 cm-10s, 0 cm-6s, and 0 cm-10s, for the simple subtraction and LIA methods. In both figures, the F value is not larger than the F critical value, so there is no statistical difference. This means that the small distances and periods do not have a major effect on the performance of the proposed method.

F-value	F crit
0.664104	3.496675
0.466751	5.518999
F value is not > F crit, so there is no significant difference.	

Figure 15: ANOVA test for the differing distance and period for simple subtraction. The results mean that minor distances and differences in the period of the PWM signal do not have a major effect on the accuracy in the control group.

F-value	F crit
3.333172	3.496675
2.345010	5.518999
F value is not > F crit, so there is no significant difference.	

Figure 16: ANOVA test for the differing distance and period for the LIA method. The results mean that minor distances and differences in the period of the PWM signal do not have a major effect on the accuracy in the proposed LIA method.

Discussions, Limitations, and Future Work:

According to the results, the reflected NIR signal in "Scenario 1" is higher than that of "Scenario 2", as the total difference in percentage between them is 2.67%, so AH1 is validated. In most experiments, the difference in the reflected NIR signals is more prominent when using the LIA method as opposed to the simple subtraction method, as the difference percentage for the LIA method is 3.46% compared to the simple subtraction method of 1.88%, so AH2 is validated.

However, there are some limitations. (i) The "orchard" box cannot completely imitate actual conditions. Future work includes adding more layers of leaves. In addition, fruits and peduncles could be shown at the same time. (ii) In the current experiment setup, ambient light is not fully blocked, which may cause minor errors, which can be addressed by adding a band-pass filter. (iii) Due to the sub-optimal quality of the current camera, further investigation into a better NIR detector will be conducted. (iv) Three statistical analysis methods, those being mean/standard deviation, t-test, and ANOVA test, are used in this study. More statistical methods will be used for comprehensive analyses in the future work. (v) In this study, only the SSM method is considered in the control group; and in the future, other information processing method could be investigated and compared with the proposed LIA method.

■ Conclusion

This research studies a combined NIR and LIA method to detect fruits fully hidden behind leaves. A very low-cost test apparatus was designed and built, using which 134 valid experiments were conducted, yielding 268 videos. Both AH1 and AH2 are supported by experiment data. The t-test shows that the proposed LIA method is effective in detecting fully occluded fruits than the SSM method. This research can significantly enhance farming operations' efficiency, such as in harvesting and yield prediction.

■ Acknowledgments

The author thanks his main research advisor, Dr. Shawn Putnam, for suggesting and explaining the method of LIA and NIR, and how it can potentially be used to detect hidden fruits, Dr. Yajie Dong for providing access to spectrophotometer equipment, and Dr. Yunjun Xu for allowing the author to use the soldering station, providing the financial support, and proofreading the manuscript.

■ Appendix A

The LIA equations relating to a sinusoid reference signal can be easily found in literatures.[15] The procedure in obtaining the LIA equation with a PWM reference signal is briefly explained here. As shown in Figure 2 (the custom designed experiment testbed), the signal A_I (with noise) goes through an average filter to remove random noise, which becomes S_I. Then it is multiplied by a reference signal R (PWM) as

$$S_O = S_I R = \{A_I \sum_{i=1}^{n} \frac{4}{\pi(2i-1)} \sin[(2i-1)\omega t + \phi] + N_i\}\{\sum_{i=1}^{n} \frac{4}{\pi(2i-1)} \sin[(2i-1)\omega t]\}$$
$$= (\frac{4}{\pi})^2 A_I \sum_{n=1,3,5,\ldots}^{\infty} \sum_{m=1,3,5,\ldots}^{\infty} \frac{1}{mn} \sin(n\omega t)\sin(m\omega t) + \frac{4}{\pi} N(t) \sum_{m=1,3,5}^{\infty} \frac{1}{m} \sin m\omega t \quad \text{(A1)}$$

DOI: 10.36838/v8i2.1

In Eq. (A1), the second term will be removed by a low pass filter to obtain its DC component S_{OL}. This DC component is the same as the reflected signal without noise, meaning A_I=S_{OL}. This result is well known; however, the detailed derivation seems not readily available in open literature. Interested readers may reach out to the author for the detailed derivation.

Note 1: The constant coefficient in A_I=S_{OL} does not affect the arguments in the Section of "Results and Discussion," as the results are based solely on the ratio.

References

1. Gené-Mola, J., Ferrer-Ferrer, M., Gregorio, E., Blok, P. M., Hemming, J., Morros, J., Rosell-Polo, J. R., Vilaplana, V., Ruiz-Hidalgo, J., Looking behind occlusions: A study on a modal segmentation for robust on-tree apple fruit size estimation. *Computers and Electronics in Agriculture* **2023**, *209*, 107854. DOI: doi.org/10.1016/j.compag.2023.107854
2. Lu, R., Beers, R. V., Saeys, W., Li, C., Cen, H., Measurement of optical properties of fruits and vegetables: A review. *Postharvest Biology and Technology*, **2020**, *159*, 111003. DOI: doi.org/10.1016/j.postharvbio.2019.111003
3. Mishra R., Karimi D., Ehsani R., Lee W. S., Identification of citrus greening (HLB) using a VIS-NIR spectroscopy technique. *The ASABE Annual International Meeting*, **2012**, *55*, 711-720. DOI: doi.org/10.13031/2013.41369
4. Kusumastuti, R. D., Van Donk, D. P., Teunter, R., Crop-related harvesting and processing planning: a review. *International Journal of Production Economics*, **2016**, *174*, 76-92. DOI: doi.org/10.1016/j.ijpe.2016.01.010
5. *Farm Labor*; Economic Research Service, USDA, revised August 2025. https://www.ers.usda.gov/topics/farm-economy/farm-labor
6. Gongal, A., Amatya, S., Karkee, M., Zhang, Q., Lewis, K., Sensors and systems for fruit detection and localization: A review. *Computers and Electronics in Agriculture*, **2015**, *116*, 8-19 DOI: doi.org/10.1016/j.compag.2015.05.021
7. Choi, D., Lee, W. K., Schueller, J. K., Ehsani, R., Roka, F., Diamond, J., A performance comparison of RGB, NIR, and depth images in immature citrus detection using deep learning algorithms for yield prediction. *The ASABE Annual International Meeting*, **2017**, 1700076. DOI: doi:10.13031/aim.201700076
8. Mahmud, M. S., Zahid, A., He, L., Choi, D., Krawczyk, G., Zhu, H., LiDAR-sensed tree canopy correction in uneven terrain conditions using a sensor fusion approach for precision sprayers. *Computers and Electronics in Agriculture*, **2021**, 191, 106565. DOI: doi.org/10.1016/j.compag.2021.106565
9. Mirbod, O., Choi, D., Heinemann, P. H., Marini, R. P., He, L., On-tree apple fruit size estimation using stereo vision with deep learning-based occlusion handling. *Biosystems Engineering*, **2023**, 226, 27-42. DOI: doi.org/10.1016/j.biosystemseng.2022.12.008
10. Mirbod O., Choi, D., Thomas, R., He, L., Overcurrent-driven LEDs for consistent image colour and brightness in agricultural machine vision applications. *Computers and Electronics in Agriculture*, **2021**, 187, 106266. DOI: doi.org/10.1016/j.compag.2021.106266
11. Wang, J., He, D., Song, J., Dou, H., Du, W., Non-destructive measurement of chlorophyll in tomato leaves using spectral transmittance. *IJABE*, **2015**, 8, 73-78. DOI: http://doi.org/10.3965/j.ijabe.20150805.1931
12. Yamamoto, K., Guo, W., Yoshioka, Y., Ninomiya, S., On plant detection of intact tomato fruits using image analysis and machine learning methods. *Sensors*, **2014**, 14, 12191-12206. DOI: https://doi.org/10.3390/s140712191
13. Shi, Y., Ma, Y., Geng, L., Apple detection via near-field MIMO-SAR imaging: a multi-scale and context aware approach, *Sensors*, **2025**, 25, 1536. DOI: https://doi.org/10.3390/s25051536
14. Shiraz, Z., Khan, U. M., Shahzad, M., FruitSight: a millimeter wave radar based approach to detect occluded fruits, *2024 IEEE 21st International Conference on Mobile Ad-Hoc and Smart Systems*, **2024**. DOI: https://doi.org/10.1109/MASS62177.2024.00044
15. Low Level Optical Detection Using Lock-in Amplifier Techniques. *PerkinElmerTM Instruments*, 1–8. chem.ucla.edu.
16. Cuccia, D. J., Bevilacqua, F., Durkin, A. J., Tromberg, B. J., Modulated imaging: quantitative analysis and tomography of turbid media in the spatial-frequency domain. *Optics Letters*, **2005**, 30, 1354-1356. DOI: doi.org/10.1364/OL.30.001354
17. Mathworld. *Fourier Series — Square Wave*. https://mathworld.wolfram.com/FourierSeriesSquareWave.html
18. MATLAB, www.MathWorks.com, last accessed on 9/16/2024.

Authors

Aiden Xu is a high school student at the Winter Springs High School, Winter Springs, FL. He is interested in conducting different types of research during his spare time and has been participating in the Science and Engineering Fair since 6th grade.